# *Ab-initio* study of MgSe self-interstitial ($Mg_i$ and $Se_i$)

Emmanuel. Igumbor[12,a*] ,Kingsley Obodo[1,b] and Water E. Meyer[1,c*]

[1]Department of Physics, University of Pretoria, Pretoria 0002, South Africa.

[2]Department of Mathematics and Physical Sciences, Samuel Adebgoyega University, Ogwa Edo, Nigeria.

[a]elgumuk@gmail.com, [b]obodokingsley@gmail.com, [c]wmeyer@up.ac.za

**Keywords:** interstitial, defect, charge state.

**Abstract.** We present detailed calculations of formation and thermodynamics transition state energies of $Mg_i$ and $Se_i$ interstitial defects in MgSe using generalized gradient approximation (GGA) and local density approximation (LDA) functional in the frame work of density functional theory (DFT). For both LDA and GGA the formation energies of $Mg_i$ and $Se_i$ are relatively low in all the configurations. The most stable Se interstitial was the tetrahedral (T) configuration having lower formation energy than the decagonal (D) configuration. The $Mg_i$ and $Se_i$ defect introduced transition state levels that had either donor or acceptor levels within the band gap. $Se_i$ acts as a donor or an acceptor and creates levels that were either deep or shallow depending on the configuration. $Se_i$ exhibit *negative-U* properties and show charge states metastability in the D configuration. $Mg_i$ acts as only shallow donor $(+2/+1)$ in both T and D configurations, in addition we pointed out the role of $Mg_i$ as electrically activating donor.

## Introduction

The semiconductor materials of magnesium and group VI (Se, Te) elements are continuously attracting scientific attention in recent years due to their wide and direct band gap. They are used in various commercial applications in electronics, visual displays high density optical memories, solid state laser devices, photo detectors [1, 2]. MgSe crystallizes in the zinc-blende (ZB), wurzite (WZ) and rock-salt (RS) structures [3]. The possible stable ground state structure of MgSe is the ZB [4]. The electronic and thermodynamic properties of MgSe in different structural phases predicting the direct band gaps and optical properties have been studied both theoretical and experimentally [6, 7]. Several authors have investigated the electronic [5], structural [8] and phonon properties [9, 10] of MgSe. Intentional doping of MgSe serves as an avenue to introduce charge carriers, which would lead to the modification of its electronic properties. To the best of our knowledge, a detailed investigation on $Mg_i$ and $Se_i$ interstitial is lacking. In this work, we present Density functional theory (DFT) calculation of the electronic properties of $Mg_i$ and $Se_i$ (hexagonal (H), decagonal (D) and tetrahedral(T) configurations) interstitial in ZB structure of MgSe. We evaluated the accuracy and precision of local density approximation (LDA) [11] and generalized gradient approximation (GGA) [12] on these systems to extract qualitative trends. The most stable configuration, thermodynamic transition levels and formation energies are presented. The rest of this paper is organized as follows: in Section II, we presented a description of the computational methodology. The results and discussion were presented in Section III . Finally, we make our concluding remarks in Section IV.

## Methodology

DFT electronic structure calculations are performed in the Vienna Ab initio Simulation Package (VASP) [13, 14]. The PAW approach of Blochl in the implementation of Kresse and Joubert was

used to describe the electron wave functions [14, 15, 16]. The semi-core and valence electrons of the MgSe are represented by plane waves. The calculations were carried out using the GGA-(PBE and PBEsol) and LDA to describe the exchange-correlation functional. For the bulk system, geometry optimization of MgSe structure was performed in the primitive unit cell using $8^3$ Monkhorst-Pack [17] k-points Brillouin zone sampling scheme and cutoff energy of 300 eV. The structure was deemed to have converged when the forces on all the atoms were less than 0.01 eV/. The calculations of the band structure was performed using the conventional unit cell employing a $8^3$ k-points in all the functional. For the pristine systems, we employed 128-atom supercells using $2^3$ Monkhorst-Pack [17] special k-points Brillouin zone sampling scheme. The total energy is adequately converged using a plane wave cut off of 600 eV. Spin orbit splitting was taken into account in all the calculations involving charge states. To calculate the defect energy of formation ($E^f$) and transition energy ($\epsilon(q/q')$) levels, we calculated the total energy E$(d, q)$ for a supercell containing the optimized defect $d$ in its charge state $q$. The defect formation energy E$^f(d, q)$ as a function of electron Fermi energy ($\varepsilon_F$) as well as the atomic chemical potentials $\mu$ is given as

$$E^f(d,q) = E(d,q) - E(pure) + \sum_i \triangle(n)_i \mu_i + q[E_V + \varepsilon_F + \triangle V], \tag{1}$$

where $\triangle(n)_i$ is the difference in the number of the constituent atoms of type $i$ between the supercells and $E_V$ is the Valence band maximum (VBM). The finite-size effects within the supercell was taken into account. This was accounted for by including the electrostatic potential alignment $\triangle V$. The defect transition energy level $\epsilon(q/q')$ is the Fermi energy, which the formation energy of charge state $q$ equals that of charge state $q'$ is given as

$$\epsilon(q/q') = \frac{E^f(d,q;\ \varepsilon_F = 0) - E^f(d,q';\ \varepsilon_F = 0)}{q' - q} \tag{2}$$

## Results and Discussion

**Structural properties of MgSe;** Using LDA, PBE and PBEsol, we obtained 5.99 lattice parameter, which was in close agreement with the experimental [3] result of 5.89 . Our computational results were in reasonable agreement with previous computation and experimental data [5, 18, 19]. For LDA, PBE and PBEsol, the calculated Kohn-Sham band gap of 2.44, 2.56 and 2.42 eV respectively were underestimated, which is consistent with other theoretical results [20, 21, 22]. To improve the band gap we have calculated the quasiparticle $E_g^Q$ band gap. The quasiparticle $E_g^Q$ band gap of 2.94, 3.02 and 2.79 eV as predicted by LDA, PBE and PBEsol resulted in slight improvement compared to the $E_g^{ks}$ as predicted by the various functionals.

**Properties and energetics of Se$_i$ and Mg$_i$:** For the optimized Se$_i$ defects, we find two competing geometric interstitial sites: the tetrahedral (T) and the decagonal (D), both lying in the $110 - plane$. The geometric structures are shown in Fig. 1. In the T configuration, the Se was bonded to four Mg atoms making it fourfold coordinated. After relaxation, the calculated bond length between Se$_i$ and Mg atoms were approximately 2.6 Å, which is 0.1 Å less than the bulk bond length. For the D configuration, after relaxation Se atom was bonded to 6 nearest Mg with bond length of 2.92 Å, while the Se-Se distance was 2.94 Å. For the optimized Mg$_i$ defect, similar interstitial site of Se$_i$ were found lying in the $110 - plane$. Similar to Se$_i$, the Mg$_i$ defect atom was bonded to nearest Se and Mg atoms having 4 and 10 fold coordination for the T and D configuration respectively. For the T after relaxation, the calculated bond length between Se$_i$ and Mg atoms were approximately 2.6 Å, which is 0.1 Å less than the bulk bond length. The Mg-Se bond lengths were approximately 2.92 Å for the D configuration. All the different

functionals gave approximately the same bond length for both $Mg_i$ and $Se_i$ interstitials in their different configurations.

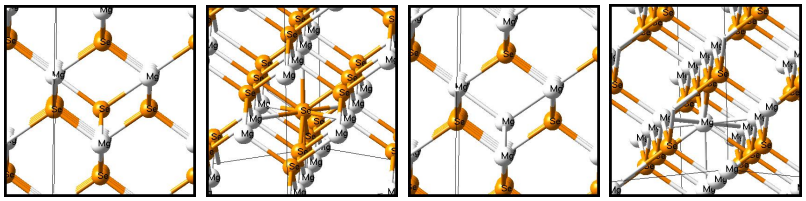

Fig. 1: Relaxed geometric structures of different configurations of $Se_i$ and $Mg_i$ interstitial in MgSe. In the following order from left, T and D configuration of $Se_i$ followed by the T and D configuration of $Mg_i$

**Se interstitial ($Se_i$) in MgSe:** Table 1 shows the calculated formation energies of $-2$, $-1$, 0, $+1$ and $+2$ charge states of $Se_i$ for the T and D configurations. For all charge states except the $-2$ charge state, the T configuration had a lower energy of formation. For the $-2$ charge state, both PBE and PBEsol predicted lower formation energy for the D configuration, while the LDA still predicted that the T charge state had the lower formation energy. For all the functionals, the formation energies increase from double positive to double negative charge states. In Fig 2, we show the plot of formation energy $E^f$, as a function of the Fermi energy with reference to the VBM using different functionals. For the T configuration, the defect introduced acceptor levels, the energy levels are displayed in Table 2. In addition to the acceptor levels created, there were donor levels at $\epsilon(+2/+1)$ and $\epsilon(+1/0)$ located at the lower half of the band gap, within 1 eV of the valence band . All three functionals predicted two deep levels. All three functionals predicted a $\epsilon(+1/0)$ transition level in the lower half of the band gap. For LDA this level is at 0.8 eV, while for PBE and PBEsol, the level was very close to the valence band. Further more all three functionals predicted a $\epsilon(0/-1)$ and $\epsilon(-1/-2)$ transition near the conduction band. For LDA these levels lie very close to the conduction band, while for PBE and PBEsol these levels were far away from the band edges. For the D configuration, the same trend of

Table 1: The formation energies $E^f$ in eV at $\varepsilon_f = 0$ for T and D configurations of $Se_i$ in MgSe using LDA, PBE and PBEsol. The charge states with the lowest formation energy for each configuration in bold

| Functionals | configuration | charge states | | | | |
|---|---|---|---|---|---|---|
| | | $-2$ | $-1$ | 0 | 1 | 2 |
| LDA | T | **6.49** | **3.56** | **0.82** | **0.01** | **-0.67** |
| | D | 8.07 | 6.39 | 4.72 | 2.93 | 1.28 |
| PBE | T | 6.55 | **3.98** | **1.54** | **1.44** | **1.39** |
| | D | **5.96** | 4.93 | 4.01 | 2.96 | 2.07 |
| PBEsol | T | 6.00 | **3.60** | **1.34** | **1.22** | **1.20** |
| | D | **5.77** | 4.64 | 3.76 | 2.68 | 1.74 |

increase in energy of formation across the double positive to double negative charge states in the T configuration was also observed. The formation energy of $-2$ charge state of the D configuration was lower that the T configuration. $Se_i$ exhibit low formation energies, suggesting that Se interstitials can form easily with low energies under equilibrium condition. For the D configuration, deep levels were observed. All three functionals predicted all the transition levels to lie close to the middle of the band gap. For some transitions $negative - U$ properties were predicted. But is interesting to know that while PBE and PBEsol results revealed evidence of acceptor level of energies 1.10 and 1.13 eV for $\epsilon(-1/-2)$ respectively, LDA did not.

While there was no sign of metastability of $Se_i$ using LDA, PBE and PBEsol predicted the $Se_i$ to show charge state metastability. This indicates that, even though the two configurations of the $Se_i$ defect had the same number and type of atoms, the stability of one configuration over the other is charge-state dependent. The deep levels observed are all in the middle of the band gap, in *n-type*, under equilibrium conditions, the $Se_i$ will be in the $-2$ charge state, and relaxed to the D configuration. Since all the transition levels due to the D configuration are mid-gap level, carrier emission from these levels will occur very slowly. In addition the electrons that are mainly concentrated at the mid-gap as a result of $Se_i$ in the MgSe shows the properties of deep donor level leading to a $DX$ center. This center can lead to the displacement of impurity or host atom. The formation of a $DX$center leads to the self compensation of a shallow donor through the formation of an acceptor state, represented by equation 3 [23]

$$2d^0 \longrightarrow d^+ + DX^-, \tag{3}$$

where $d^0$ is the donor impurity in the neutral charge state, $d^+$ is the positively charged donor, and $DX^-$ represents the impurity in the negatively charged $DX$ configuration. The effective correlation energy ($U^{eff}$) associated with this reaction is defined as

$$U^{eff} = E^{+1} + E^{-1} - 2E^0, \tag{4}$$

where $E^0$ and $E^+$ are the formation energies of the neutral and the donor impurity in the positive charge states, and $E^-$ is the formation energy of the negatively charged DX configuration. A *negative*$-U$ defect occurs when an ionized defect captures two electrons with the second electron being more tightly bound that the first. This probably results from lattice relaxations and gives rise to metastability. We have obtained the $U^{eff}$ of $-$ 0.20 eV using PBEsol $-$ 0.12 eV using LDA and $-$ 0.13 eV using PBE. Our electronic structure calculation indeed show that the impurities that give rise to shallow defect levels also give rise to states that are resonant either in the conduction band for donors or in the valence band for acceptors.

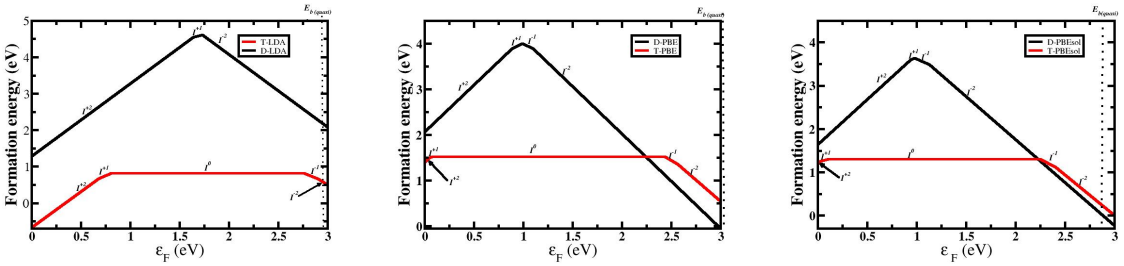


Fig. 2: Plot of formation energy and Fermi energies of $Se_i$ in MgSe. The labels indicate various charge states. The gap is in the following order from left: LDA, PBE and PBEsol.

Table 2: The thermodynamic transition charge state levels $\epsilon(q/q')$ above $E_V$ (eV) for T and D configurations of $Se_i$ in MgSe using LDA, PBE and PBEsol.

| | | (+2/+1) | (+1/0) | (0/-1) | (-1/-2) | (+1/-1) | (+1/-2) |
|---|---|---|---|---|---|---|---|
| LDA | T | 0.68 | 0.81 | 2.76 | 2.91 | - | - |
| | D | 1.64 | - | - | - | - | 1.74 |
| PBE | T | 0.05 | 0.08 | 2.44 | 2.54 | - | - |
| | D | 0.88 | - | - | 1.10 | 0.99 | - |
| PBEsol | T | 0.03 | 0.11 | 2.26 | 2.40 | - | - |
| | D | 0.94 | - | - | 1.13 | 0.98 | - |

Table 3: The formation energies $E^f$ in eV at $\varepsilon_f = 0$ for T and D configurations of $Mg_i$ in MgSe using LDA, PBE and PBEsol. The configurations with the lowest formation energy in bold

| Functionals | configuration | charge states | | | | |
|---|---|---|---|---|---|---|
| | | −2 | −1 | 0 | +1 | +2 |
| LDA | T | **13.41** | **9.69** | 6.30 | 2.80 | 0.29 |
| | D | 13.85 | 10.02 | **6.13** | **2.16** | **-1.16** |
| PBE | T | **11.73** | **8.48** | **5.30** | **1.87** | **-1.10** |
| | D | 11.76 | 8.49 | 5.31 | 1.90 | -0.90 |
| PBEsol | T | **10.94** | **7.79** | 4.67 | **1.32** | 1.49 |
| | D | 11.41 | 7.90 | **4.66** | 1.36 | **-1.27** |

**Mg interstitial ($Mg_i$) in MgSe:**

Table 3 shows the calculated formation energies of −2, −1, 0, +1 and +2 charges of $Mg_i$ in the T and D configurations. In $Mg_i$, the formation energy predicted by PBE is lower in the D configuration, implying that this structure is more stable than the T. While using LDA and PBEsol, the T configuration charge states formation energy is lower in the negative charge states. The formation energy in this configuration is relatively low. In Fig 3, we shown the plot of energy of formation as a function of the Fermi energy using different functionals.

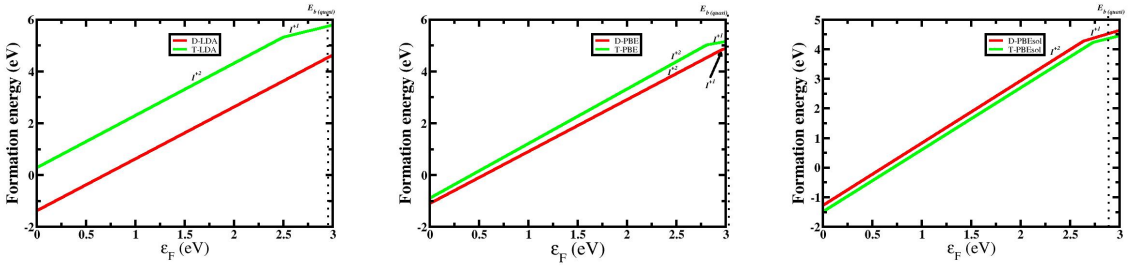


Fig. 3: Plot of formation energy as a function of Fermi energy of $Mg_i$ in MgSe. The labels indicate various charge states. The gap is in the following order from left: LDA, PBE and PBEsol.

Table 4: The thermodynamic transition charge state levels $\epsilon(q/q')$ above $E_V$ (eV) for T and D configurations of $Mg_i$ in MgSe using LDA, PBE and PBEsol.

| | | (+2/+1) | (+1/0) |
|---|---|---|---|
| LDA | T | 2.50 | - |
| | D | - | - |
| PBE | T | 2.97 | - |
| | D | 2.81 | |
| PBEsol | T | 2.81 | - |
| | D | 2.64 | - |

For the T configuration, all three functionals predicted transition state levels of (+2/+1), close to the conduction band at 2.50, 2.97 and 2.81 eV using LDA, PBE, and PBEsol respectively. The transition states energy levels were displayed in Table 4 . In all the functionals, there was no evidence of acceptor level, this is in contrasts to the acceptor levels found in the T configuration of $Se_i$. In the D configuration, there was an increase in the formation energies from the double positive to the double negatively charge states. The PBE and PBEsol predicted 2.81 and 2.64 eV respective donor transition state level of (+2/+1) close to the conduction band,

while LDA did not predict any transition levels in the band gap. The LDA, PBE and PBEsol predicted that there was no evidence of acceptor level and *negative*$-U$ properties, this is in contrast to the acceptor levels and *negative* $-U$ properties found in the D configuration of $Se_i$ using PBE and PBEsol. The transition levels observed in this configuration were located close to the CBM making them a shallow donor and electrons can easily be captured in the conduction band. Both LDA and PBE predicted that the D configuration is more stable for all accessible charge states, while PBEsol predicted the T configuration to be slightly more stable.

## Summary

In this study, we present detailed results of the calculated electronic, energetic properties of different configurations of $Mg_i$ and $Se_i$ in MgSe. Formation and thermodynamics transition states energies of $Mg_i$ and $Se_i$ defects in MgSe using PBE, PBEsol and LDA functional in the frame work of DFT are presented. We have shown that the formation of $Mg_i$, and $Se_i$ defects require relatively low energy. Self interstitial of MgSe introduced transition state levels that are either deep or shallow within the band gap depending on the functionals. In *p-type* material, the $Se_i$ would be more stable in the T configuration, leading to levels close to both the conduction and valence bands. In *n-type* material, both PBE and PBEsol predicted the D configuration to be more stable, with all its transition levels in the middle of the band gap. Charge state controlled metastability and *negative* $-U$ transitions were also predicted $Mg_i$ on the other hand, introduced a shallow $(+2/-1)$ transition level close to the conduction band was predicted by all three functionals in all configurations, except LDA for the D configuration. According to LDA and PBE functionals, the D configuration was most stable for all accessible charge states, while the T configuration was slightly more stable for all charge states according to PBEsol We also pointed out the properties of $DX$ center as a result of Se interstitial in the D configuration and the metastability of charge states of $Se_i$ using both PBE and PBEsol functional. We expect the data presented to be useful in the process modeling of MgSe-based devices.

## Acknowledgement

This work is based on the research supported partly by National Research foundation (NRF) of South Africa (Grant specific unique reference number (UID) 78838). The opinions, findings and conclusion expressed are those of the authors and the NRF accepts no liability whatsoever in this regards.

## References

[1] A. Waag, H. Heinke, S. Scholl, C.R. Becker, and G. Landwehr. Journal of Crystal Growth, 131(34) (1993), 607 – 611.

[2] M. W. Wang, J. F. Swenberg, M. C. Phillips, E. T. Yu, J. O. McCaldin, R. W. Grant, and T. C. McGill. Applied Physics Letters, 64(25), (1994), 3455–3457.

[3] Hiroyuki Okuyama, Kazushi Nakano, Takao Miyajima, and Katsuhiro Akimoto. Journal of Crystal Growth, 117(14), (1992), 139 – 143.

[4] G. Gkolu, M. Durandurdu, and O. Glseren. Computational Materials Science, 47(2):593 – 598, (2009).

[5] S. Duman, S. Ba˘gc ı, H. M. T¨ut¨unc¨u, and G. P. Srivastava. Phys. Rev. B, 73:205201, (2006).

[6] Ting Li, Huan Luo, Raymond G. Greene, Arthur L. Ruoff, Steven S. Trail, and Francis J. DiSalvo, Jr. Phys. Rev. Lett., 74:5232–5235, (1995).

[7] Journal of Alloys and Compounds, 609:185–191, (2014).

[8] Dinesh Varshney, N. Kaurav, U. Sharma, and R.K. Singh. Journal of Physics and Chemistry of Solids, 69(1):60–69, (2008).

[9] D. Wolverson, D. M. Bird, C. Bradford, K. A. Prior, and B. C. Cavenett. Phys. Rev. B, 64:113203, (2001).

[10] Daming Huang, Caixia Jin, Donghong Wang, Xiaohan Liu, Jie Wang, and Xun Wang. Applied Physics Letters, 67(24):3611–3613, (1995).

[11] D. M. Ceperley and B. J. Alder. Phys. Rev. Lett., 45:566–569, (1980).

[12] J. P. and Alex Zunger. Phys. Rev. B, 23:5048–5079, May 1981.

[13] G. Kresse and J. Furthmuller. Phys. Rev. B, 54:11169–11186, ( 1996).

[14] G. Kresse and D. Joubert. Phys. Rev. B, 59:1758–1775, (1999).

[15] G. Kresse and J. Furthmuller. Computational Materials Science, 6(1):15 – 50, 1996.

[16] P. E. Blochl. Phys. Rev. B, 50:17953–17979, (1994).

[17] Hendrik J. Monkhorst and James D. Pack. Phys. Rev. B, 13, (1976) 5188–5192, .

[18] D. Rached, N. Benkhettou, B. Soudini, B. Abbar, N. Sekkal, and M. Driz. physica status solidi (B), 240(3), (2003) 565–573.

[19] F. Drief, A. Tadjer, D. Mesri, and H. Aourag. Catalysis Today, 89(3), (2004)343 – 355.

[20] Ji-Hui Yang, Shiyou Chen, Hongjun Xiang, X. G. Gong, and Su-Huai Wei. Phys. Rev. B, 83 (2011), 235208.

[21] D. J. Chadi. Phys. Rev. B, 59, (1999), 15181–15183.

[22] D. J. Chadi and K. J. Chang. Phys. Rev. B, 39 (1989), 10063–10074.

[23] C. H. Park and D. J. Chadi. Phys. Rev. B, 55 (1997), 12995–13001.